Performance Assessment of Steel Isolated Structures Considering Heating in Lead Core Based on Seismic Risk

Majid Gholhaki[1*], Mehdi Banazadeh[2], and Hossein Parvini Sani[3]

1. Associate Professor in Structural Engineering, Civil Engineering College, Semnan University, Semnan, Iran, * Corresponding Author; email: mgholhaki@semnan.ac.ir
2. Associate Professor in Structural (Earthquake) Engineering, Department of Civil and Environmental Engineering, Amirkabir University of Technology (Tehran Polytechnic), Tehran, Iran
3. Ph.D. in Structural Engineering, Civil Engineering College, Semnan University, Semnan, Iran

Received: 24/05/2016
Accepted: 11/02/2017

ABSTRACT

This paper presents a methodology to utilize performance-based seismic design procedure for evaluating the effect of heating in lead core of isolated structures with lead-rubber bearing based on collapse assessment and seismic loss estimation. Nonlinear archetypes of conventional 4-story steel special moment resisting frame, isolated intermediate moment resisting frame with and without heating in lead core effect are compared with each other under far-field (FF) and near-field (NF) earthquakes. The results of this study show that heating in lead core increases collapse risk, expected annual loss (EAL) and expected annual fatalities up to 40%. Besides, it has been found that the effect of heating in lead core for isolated structures increases under NF comparing with FF ground motions. Sensitivity analysis is employed to study the effect of modeling uncertainty on the loss estimation process show that the effect of modeling uncertainty on the EAL increases for NF ground motions comparing with FF ground motions.

Keywords:
Isolated structures;
Loss estimation;
Heating in lead core;
Performance-based seismic design;
Seismic risk

1. Introduction

Performance-Based Seismic Design (PBSD) is a procedure that permits the design and construction of buildings with a realistic and reliable understanding of the risk of life, occupancy, and loss that may occur as a result of future earthquakes [1]. PBSD improves seismic risk decision-making through assessment and design methods that have a strong scientific basis and that express options in terms that enable clients to make informed decisions. The methodology needs to be supported by a consistent procedure that characterizes the important seismic hazard and engineering aspects of the problem, and that relates these quantitatively to the defined performance measures [2].

Strong earthquakes cause losses and disturb normal operation of structures. Seismic Isolation has proven to be an effective method of control for structures during seismic events and mitigating seismic losses and damage costs [3-4]. Isolated Structure tends to respond like rigid mass in a way that majority deformations can take place in the flexible layer of the isolator [5]. Isolated structures as well as fixed structures could suffer from inelastic deformation and serious damage under intense

seismic ground motions [6]. Moreover, the effects of near-field earthquake with large velocity pulses can bring the seismic isolation devices to critical conditions [7].

Elastomeric bearings that are used in isolation system can be divided into three sub-categories: lead rubber (LR), high-damping rubber (HDR) and natural rubber. Lead rubber bearings generally consist of natural rubber bearings with a lead core press-fit into the central mandrel hole [5]. The strength degradation of LR bearings due to the heating in lead core under cyclic shear loading has already been validated by Kalpakidis et al [8].

This study investigates the characteristics of seismic performance of inelastic isolated structures with the effect of heating in lead core subjected to set of far-field (FF) and near-field (NF) ground motion records, and then evaluates the isolated structures from loss estimation standpoint. PBSD provides a useful framework for developing an understanding of the relationships among the characteristics of the ground motion, superstructure and isolation system, and to evaluate the ability of various design approaches and isolator system properties to reliably reach targeted performance states [9]. Seismic loss estimation methods combine seismic hazard, structural response, damage fragility, and damage consequences to allow quantification of seismic risk based on seismic performance of a building that is expressed as the probable damage and resulting consequences of a building's response to earthquake shaking [10-11].

The benefit of such an approach is an advanced method to assess the effect of heating in lead core on isolation system performance in terms of loss estimation. The analysis results show that seismic isolation reduces collapse probability in super-structures significantly and can be cost-effective in mitigating seismic risk; however, heating in lead core increases seismic collapse up to 40%. Besides, the effect of heating in lead core on increasing expected annual loss and expected annual fatalities is remarkable. Furthermore, this effect on seismic risk under NF earthquakes is greater than FF earthquakes.

2. Design and Modeling Assumptions for the Buildings

2.1. Design Assumptions

A 4-story conventional and base-isolated moment-resisting frame archetypes that are designed by ETABS 2015 software are considered as the case studies in this paper. These commercial offices (risk category III and seismic importance factor I =1.25) were designed by the equivalent lateral force method for conventional building and response-spectrum method for base-isolated building to meet the requirements of ASCE 7-10 [12] and AISC 360-10 [13]. The buildings were located in Los Angeles, California, on stiff soil (site class *D*) with mapped spectral accelerations S_s =2.111g for short periods and S_1 = 0.733g for a 1-s period (g = gravitational acceleration).

The conventional building was detailed for high ductility as a special moment-resisting frame (SMF) and uses reduced beam section (RBS) connections, which are prequalified according to AISC 341-10 [14]. However, the isolated building, which has lower ductility requirements, was detailed as an isolated intermediate moment-resisting frame (I-IMF) using welded unreinforced flange, welded web (WUF-W) beam-column connections. Response modification factors were R=8 for the SMF, and R=2 for the I-IMF, assuming a design yield strength of 345 MPa for structural steel. Design drift limits were 2% for the SMF and 1.5% for the I-IMF.

The archetypes are 55 by 55 meters in plan, with bottom story height of 5.48 meters, typical story heights of 4.57 meters and column spacing of 9.15 meters in each direction as depicted in Figure (1). Lateral resistance is provided by two 6-bay perimeter moment frames in the X-direction and two 4-bay perimeter and one 4-bay interior moment frames in the Y-direction; moment-resisting bays. The steel sections selected for the moment-resisting frame members are listed in Table (1).

The design displacement DD of the isolators in the design earthquake and the maximum displacement DM in the MCE at the center of rigidity are computed as [12]:

$$D_D = \frac{gS_{D1}.T_D}{4\pi^2 B_D} \quad (1)$$

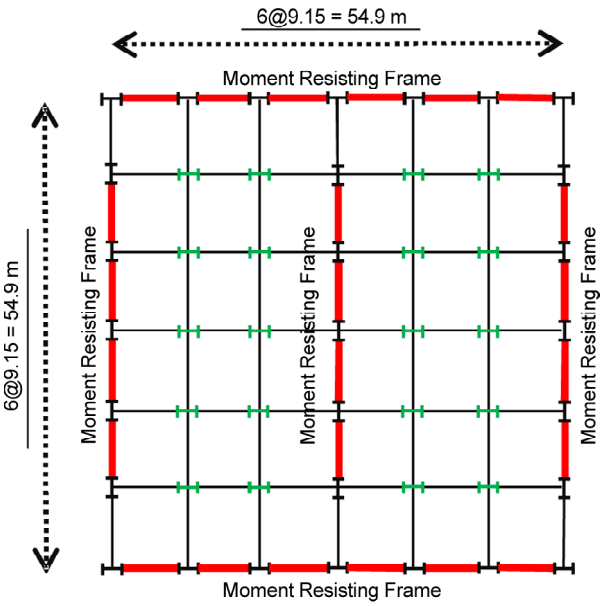

Figure 1. Plan layout of the archetypes .

Table 1. Design outcomes for the beams and columns of the SMF and I-IMF.

Frame	Story	Columns	Beams
SMF	Roof	W14×233	W30×108
	3	W14×370	W33×130
	1&2	W14×398	W33×152
I-IMF	Roof	W14×233	W27×102
	3	W14×283	W30×108
	1&2	W14×370	W33×141

$$D_M = \frac{gS_{M1}.T_M}{4\pi^2 B_M} \tag{2}$$

where T_D, T_M = effective isolation periods; B_D, B_M coefficients that modify the spectrum for damping; and S_{D1}, S_{M1} = 1-s spectral accelerations for the corresponding events. The isolation devices have been designed in detail using Lead-Rubber Bearing (LR) by iteration as listed in Table (2).

Detailed three-dimensional (3D) numerical models of the structures were developed in OpenSees software, open-source analysis platform. Although the buildings are symmetric about both axes, the mass centers were shifted by 5% of the longest plan dimension in both directions to account for accidental torsion. Slab action was accounted for a rigid diaphragm, except at the base level of the I-IMF, where slabs were modeled with shell elements to enhance the rigidity of the model against local isolator uplift [15-16].

Table 2. Characteristics of the Lead-Rubber Bearing (LRB).

Characteristics	Value
Outer Diameter [cm]	80
Diameter of Lead [cm]	14
Total Height of Rubber Layers [cm]	20
Number of Rubber Layers	37
Thickness of One Rubber layer [cm]	0.54
Thickness of One Steel Plate [cm]	0.44
Total Height [cm]	42.22
Characteristic Strength [kN]	123
Initial Stiffness [kN/m]	12800
Post Yield Stiffness [kN/m]	984
Equivalent Shear Stiffness [kN/m]	1600
Equivalent Damping Ratio (%)	23.2

Moment-resisting frame modeled using lumped plasticity elements [17]. The rotational springs at the member ends are idealized by the Ibarra-Medina-Krawinkler (IMK) model [18] as this was modified by Lignos and Krawinkler [19] to incorporate asymmetric component hysteretic behavior as well as ultimate deformation rotation. To determine their properties, they fitted a database of structural tests using regression equations that incorporate the effect of material, section geometry and member dimensions. This database is available in the following link: http://dimitrios-lignos.research.mcgill.ca/databases/.

The steel stress-strain and moment-curvature relationships were assumed to be bilinear, with a strain hardening ratio of 3%. Gravity beams were modeled using elastic frame elements with moment releases at both ends. In the SMF, moment-resisting and gravity columns were fixed and pinned at the base, respectively; whereas in the I-IMF, moment connections were assumed at all base level beam column joints.

Energy dissipation was applied to the conventional structure and the isolated superstructure using stiffness proportional damping calibrated to give 2.5% damping at their respective first mode frequencies. Stiffness proportional damping was selected since Rayleigh damping has been observed to artificially suppress the first mode of an isolated building even compared with a rigid structure approximation. Tangent stiffness proportional damping rather than initial stiffness proportional damping was selected to prevent the damping forces from becoming unrealistically large compared with the element forces after the superstructure yields [16].

2.2. Ground Motions Selection

The approach requires a set of records that can be used for incremental dynamic analysis of buildings and evaluation process [20]. In this study FF record set includes twenty-two records (44 individual components) and the NF record set includes twenty-eight records (56 individual components) selected from the PEER NGA database based on FEMA P695 [21]. Seismic parameter of selected ground motions are listed in Table (3). The intensity measure (IM) for representing the intensity parameter and scaling the ground motions is selected to be the spectral acceleration at the first mode period with 5% coefficient of damping ($S_a(T_1,5\%)$).

2.3. Modeling of Base Isolation Element in OpenSees

Isolators were modeled independently, one beneath each column, using a LeadRubberX element in OpenSees software. The physical model of an elastomeric bearing is considered as a two-node, twelve degrees-of-freedom discrete element. The two nodes are connected by six springs that represent the mechanical behavior in the six basic directions of a bearing. This model of LRB bearings is presented for the analysis of base isolated structure under design and beyond design basis shaking, explicitly considering both the effects of lateral displacement and cyclic vertical and horizontal loading [22].

For LR bearings, the effective yield stress of lead is not constant but decreases with number of cycles because of the heating of the lead-core under large cyclic displacements. The extent of reduction depends on the geometric properties of bearing and speed of motion. Kalpakidis et al [8] proposed the dependence of characteristic strength of LR bearings on the increase in the temperature of lead-core which itself is a function of time. Kumar et al [22] developed LeadRubberX element in OpenSees software that can capture strength degradation in cyclic shear loading due to heating of lead core, which is used for studying the effect of lead core heating on archetype named "I-IMF-Heat".

3. Collapse Assessment and Loss Estimation

3.1. Collapse Assessment Results

Tables (4) and (5) presents collapse assessment results for FF and NF ground motion respectively. In these tables T_1(s) is the first mode period, $[S_a]_{collapse}$ is collapse spectral acceleration (g), $S_{a2/50}[T_1]$ is the spectral acceleration with 2% probability of exceedance in 50 years (g), $P[C|Sa_{MCE}]$ is the probability of collapse at the maximum considered spectral acceleration, $\lambda_{collapse}$ is the result of integration of collapse fragility function together with

Table 3. Seismic Parameters of selected ground motions.

Parameter Value	Far-Field Ground Motions			Near-Field Ground Motions		
	Max	Ave	Min	Max	Ave	Min
Magnitude	7.6	7	6.5	7.9	7	6.5
PGA_{max} (g)	0.82	0.43	0.21	1.43	0.6	0.22
PGV_{max} (cm/s)	115	46	19	167	84	30
Site-to Source Epicentral Distance (km)	26.4	16.4	11.1	8.8	4.2	1.7

Table 4. Summary of IDA results for FF ground motions.

Type of Building	T_1(s)	$[S_a]_{collapse}$	$Sa_{2/50}[T_1]$	$P[C\|Sa_{MCE}]$	$\lambda_{collapse}[\times10^{-4}]$	CMR	σ_{RTR}	RDR_{col}	IDR_{col}
SMF	1.42	1.78	0.749	0.125	0.943	2.38	0.44	0.043	0.043
I-IMF	2.77	1.64	0.394	0.002	0.157	4.16	0.48	0.032	0.034
I-IMF-Heat	2.77	1.46	0.394	0.0031	0.204	3.71	0.49	0.038	0.038

Table 5. Summary of IDA results for NF ground motions.

Type of Building	T_1(s)	$[S_a]_{collapse}$	$Sa_{2/50}[T_1]$	$P[C\|Sa_{MCE}]$	$\lambda_{collapse}[\times10^{-4}]$	CMR	σ_{RTR}	RDR_{col}	IDR_{col}
SMF	1.42	1.69	0.749	0.1380	1.507	2.26	0.48	0.061	0.062
I-IMF	2.77	1.45	0.394	0.0049	0.296	3.68	0.45	0.044	0.045
I-IMF-Heat	2.77	1.23	0.394	0.0081	0.414	3.12	0.46	0.048	0.049

site specific hazard curve, collapse margin ratio (CMR) defined as the ratio of the median of collapse spectral acceleration to the spectral acceleration with 2% probability of exceedance in 50 years, σ_{RTR} is the record-to-record dispersion resulted from the variety in the values of the collapse spectral acceleration due to the different spectral shapes of the set of records, RDR_{col} and IDR_{col} are respectively roof drift ratio and maximum interstory drift ratio at collapse.

Figures (2) and (3) show the collapse fragility curves for all archetypes for FF and NF ground motions, respectively. The horizontal axis is normalized with $S_{a[2/50]}$. It can be seen, the effect of heating in lead core on collapse fragility under FF ground motions in low spectral accelerations is negligible; however, in high spectral accelerations this effect is remarkable. In addition, the effect of heating in lead core in collapse fragility under NF ground motions for all range of spectral acceleration is considerable, but in high spectral acceleration this effect is reduced.

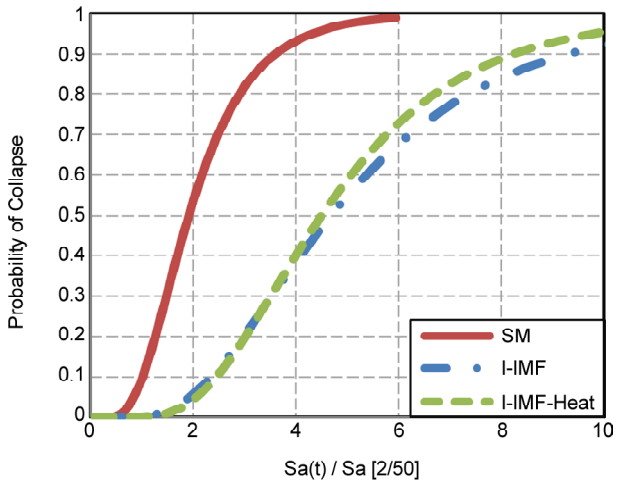

Figure 2. The lognormal collapse fragility for FF ground motions.

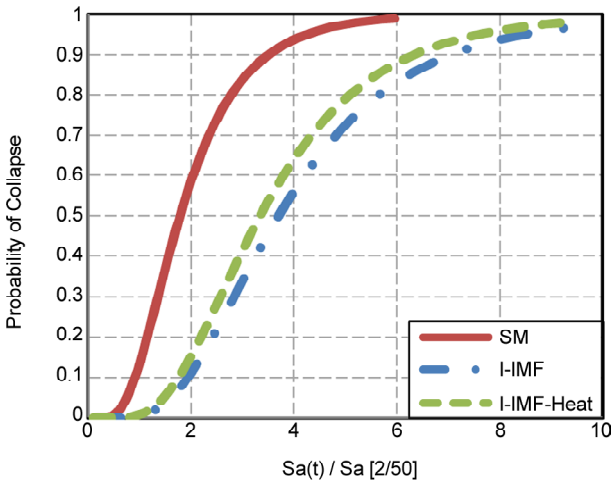

Figure 3. The lognormal collapse fragility for NF ground motions.

Annual frequency of collapse ($\lambda_{collapse}$) is the most useful measure to compare collapse safety of different archetypes as it considered both collapse fragility curve of structure and hazard curve of the location that can be obtained from USGS: http://geohazards.usgs.gov/hazardtool/application.php. Considering heating effect on archetypes (I-IMF-Heat) in Tables (4) and (5), it can be seen that the $\lambda_{collapse}$ increases by 30% under FF ground motions and 40% under NF ground motions, also the CMR reduces by 10.8% under the FF ground motions and 15.2% under the NF ground motions. Therefore, the effect of heating in lead core on decreasing the CMR and increasing the $\lambda_{collapse}$ in the NF is greater than FF earthquakes. Moreover, the effect of heating in lead core increases RDR_{col} and IDR_{col} under the FF and NF earthquakes.

3.2. Loss Estimation

Collapse assessment is not adequate for comparing seismic safety in structures [23] because variations in accelerations, velocities and drifts developed in stories, differences in number of occupants and their distribution and the monetary value of the continents cause buildings to suffer from different levels of human and monetary losses during a seismic event [24]. Performance assessment calculation tool (PACT) has been used in the seismic performance and loss estimation of buildings [24-27]. PACT 2 and the approach of loss estimation of PBSD in FEMA P-58 [1] is utilized in this study to evaluate human losses and the cost and time that shall be allocated for the renovation of seismic-induced damages. This method relies on fragility curves to define the earthquake-induced damages to structural and non-structural components. By having engineering demand parameter (*EDP*) as the drift or acceleration or velocity induced in each story by earthquake, the method gives the probability of exceedance of a particular damage state in the related component ($P[DM|EDP]$). Having the damage states and by employing consequence functions, decision variables (*DV*) as probable

financial and human losses can be evaluated ($P[DV|DM]$). Using the total probability theorem, the mean annual occurrence rate of the decision variable $\lambda[DV]$ can be found by integrating $P[DV|DM]$, $P[DM|EDP]$ and $P[EDP|IM]$ obtained from structural analysis and the mean annual frequency of exceedance of the intensity $\lambda[DV]$ simultaneously. Framework formula for loss estimation expressed as follows [28]:

$$\lambda[DV] = \iiint P(DV \mid DM)\,P(DM \mid EDP)\,P(EDP \mid IM)\,\lambda(IM)\,.\,dDM.\,dEDP.\,dIM \tag{3}$$

The decision variables (DV) in this study are defined as expected annualized repair cost or financial losses (EAL), expected annualized repair time (EAT), expected annualized fatalities (EAF) and expected annualized injuries (EAI), which are defined as the average values of these parameters that are expected to occur annually. These metrics are obtained by integrating the diagram of expected decision variable [$E(DV)$] versus intensity together with site-specific hazard curve and is interpreted as the estimated loss that occurs on average every year. It should be noted that precise quantification of performance measures is impossible, thus probabilistic framework should be utilized. According to probability theorem, final loss can be obtained from Eq. (3) considering the two probable cases, Collapse (C) and No-collapse cases:

$$E[DV/IM] = E(DV \mid IM, NC)\times(1 - P(C/IM)) + E(DV \mid IM, C)\times P(C \mid IM) \tag{4}$$

Employing the vulnerability functions, values of EAL and EAF are computed as follows:

$$EAL = \lambda_0 \iiint E[RC/IM]\,P[IM \mid IM \geq im_0]\,dIM \tag{5}$$

where λ_0 is the mean annual rate of events with $IM \geq im_0$, im_0 is a threshold event under which EAL or EAF is considered negligible and is considered as 2% of collapse intensity, and $P[IM \mid IM \geq im_0]$ is the conditional probability of occurrence of IM [24].

3.3. Assumptions for Loss Estimation

Before estimating loss for each archetype, some necessary assumptions must be made. Table (6) shows the list of the considered damageable components and the associated fragility and consequence functions based on NISTIR classification [29]. In this table, the dispersion of Engineering Demand Parameter (EDP) varies from 0.3 to 0.6 and the dispersion of repair cost varies from 0.1 to 0.64. In order to estimate the probable number of occupants at the time of earthquake occurrence, we used the population models of PACT 2 for commercial office, which return the number of occupants based on hour of day, day of week and month of year. To evaluate the replacement cost of each archetype, tools such as R.S. Square Foot Costs (RSMeans Building Construction Cost Data Online) from https://www.rsmeansonline.com, can be used [30]. The RS Means estimations include all of the important and most common structural and non-structural components. However, these estimations usually cover the lower bound of construction costs [24]. Replacement cost of SMF and I-IMF are estimated to be 30.6 and 35.8 million dollars, respectively.

3.4. Modeling Uncertainties

Modeling uncertainty, β_m, results from inaccuracies in component modeling, damping, and mass assumptions which can have a significant impact on the seismic performance. For the purpose of estimating β_m, these uncertainties have been associated with the level of building definition and construction quality assurance, β_c, and the quality and completeness of the nonlinear analysis model, β_q. The total modeling dispersion can be estimated as [1]:

$$\beta_m = \sqrt{\beta_c^2 + \beta_q^2} \tag{6}$$

To study the effect of modeling uncertainties in loss estimation, two cases are considered, the first case $\beta_m = 0$ (without modeling uncertainty) and the second case, $\beta_c = 0.1$ for superior quality (new buildings) and $\beta_q = 0.4$ for limited quality that are resulted in $\beta_m = 0.41$.

3.5. Loss Estimation Outcomes

Repair cost is defined here necessary to restore a building to its pre-earthquake condition, or in the case of total loss, to replace the building with a new structure of similar construction (in dollars).

Table 6. Damageable components and the associated fragility and loss parameters.

NISTIR Classification	Component Name	Unit	EDP	Damage States	Mean of Damaging EDP	Mean of the Repair Cost ($)
B1031.001	Gravity Connections	Per Connection	IDR[a]	Yielding Partial Tearing	4% 8%	10176 10376
B1031.011c	Column Base Plates	Per Connection	IDR	Initiation of Crack Propagation of Crack Complete Fracture	4% 7% 10%	17208 24976 31696
B1031.021c	Column Splices	Per Connection	IDR	Cracking of the Weld Failure of the Web Complete Fracture	4% 7% 10%	9072 13075 37688
B1035.032	Moment Connection	Per Bay	IDR	Local Buckling lateral Distortion fatigue Fracture	3% 4% 5%	35000 58500 58500
B2011.102	Exterior Walls	100 ft^2 (9.3 m^2)	IDR	Cracking Spalling Fracture	0.25% 0.52% 2.52	653 1053 3480
C1011.011a	Wall Partition	1300 ft^2 (121 m^2)	IDR	Light Cracking Moderate Cracking Severe Cracking	0.21% 0.71% 1.2%	5000 20000 32000
C3032.003d	Suspended Ceiling	2500 ft^2 (232 m^2)	PFA[b]	5% Damage 30% Damage Collapse	0.35g 0.55g 0.8g	3500 29000 55000
D1014.021	Hydraulic Elevator	Each	PGA[c]	Failure	0.4g	56000
D2021.014a	Cold Water Piping	1000 ft (305 m)	PFA	Minor Leakage Pipe Break	2.25 g 4.1 g	380 3220
D2022.023a	Hot Water Piping	1000 ft (305 m)	PFA	Minor Leakage Pipe Break	0.55 g 1.1 g	300 2600
D3041.022c	HVAC Ducting	1000 ft (305 m)	PFA	Support Fail Ducting Fall	1.5 g 2.25 g	680 6465
D3041.032c	HVAC Diffusers	10 Units	PFA	Dislodges and Falls	1.5 g	3000
D3031.011c	Chiller	Each	PFA	Inoperative	0.5 g	280720
D3031.021c	Cooling Tower	Each	PFA	Damaged Equipment	0.5 g	143220
D3041.102c	HVAC Fan	Each	PFA	Fall Out	0.7 g	2000
D4011.073a	Fire Sprinkler Drop	100 ft (30.5 m)	PFA	Leakage Breakage	0.75 g 0.95 g	500 550
D5012.031a	Distribution Panel	Each	PFA	Inoperative	0.95 g	10202
E2022.023	Desktop electronics	Each	PFA	Inoperative	0.4g	1800
E2022.106a	Bookcase	Each	PFV[d]	Collapse	0.25 m/s	4000
E2022.125a	Lateral Filing Cabinet	Each	PFV	Falls Over	0.52 m/s	4000

[a] IDR, Interstory Drift Ratio [b] PFA, Peak Ground Acceleration [c] PGA, Peak Ground Acceleration [d] PGV, Peak Ground Velocity

Table 7. Loss estimation outcomes for FF ground motions.

Type of Building	$\beta_m = 0$				$\beta_m = 0.41$			
	Normalized EAL (%)	EAT	EAF	EAI	Normalized EAL (%)	EAT	EAF	EAI
SMF	0.61	6.60	0.0068	0.086	0.64	6.77	0.0068	0.091
I-IMF	0.17	1.91	0.0010	0.026	0.19	1.98	0.0010	0.030
I-IMF-Heat	0.18	2.41	0.0012	0.027	0.21	2.52	0.0012	0.032

[a]EAT, Expected Annualized repair Time [b]EAF, Expected Annualized Fatalities [c]EAI, Expected Annualized Injuries

Casualties is outlined here Loss of life or serious injury requiring hospitalization, occurring within the building envelope and includes fatalities and injuries, and repair time is the time necessary to repair a damaged building to its pre earthquake condition. Performance measures of the FF and NF ground motions are listed in Tables (7) and (8), respectively. Besides, the EAF and EAT of these tables (with uncertainty) are depicted in Figure (4).

The expected annual loss (EAL) values normalized by replacement cost, ranging between 0.17% and 0.65%. The maximum normalized EAL is for

Table 8. Loss estimation outcomes for NF ground motions.

Type of Building	$\beta_m = 0$				$\beta_m = 0.41$			
	Normalized EAL (%)	EAT	EAF	EAI	Normalized EAL (%)	EAT	EAF	EAI
SMF	0.61	6.25	0.0088	0.090	0.65	6.65	0.0088	0.106
I-IMF	0.18	2.62	0.0020	0.040	0.21	2.72	0.0020	0.046
I-IMF-Heat	0.24	3.06	0.0027	0.043	0.29	3.20	0.0027	0.051

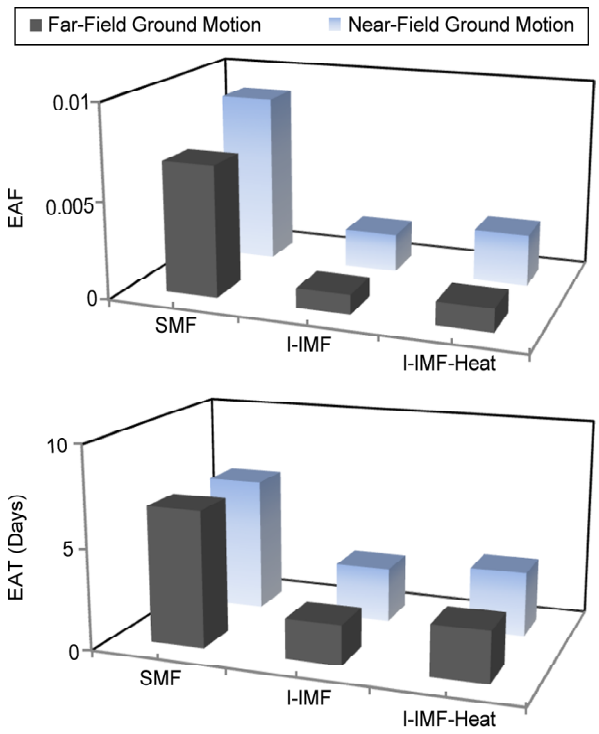

Figure 4. EAF and EAT for FF and NF ground motions.

the SMF in the NF ground motions and minimum is for I-IMF in the FF ground motions. It is evident that the EAL significantly decreases as isolation system is used and considering heating in lead core of isolated archetypes increases the EAL because of increasing EDPs like drifts. This effect increases under the NF ground motions as the percentage change in the EAL considering the heating effect with modeling uncertainty are 10.5% and 38.5% under FF and NF earthquakes, respectively.

The expected annual repair time (EAT) decreases significantly in isolated structures that emphasizes the importance of these structures for operational performance after seismic events.

The expected annual fatalities (EAF) and expected annual injuries (EAI) due to earthquake occurrence is a measure to examine to which extent the modern building codes are successful in protecting human lives against earthquake. Collapse of structures is the main source of fatalities; therefore, in this study, it is assumed that the earthquake-induced human fatalities are only the result of structural collapse. It is evident that the EAF and EAI significantly decreases as isolation system is used and heating in lead core of isolation system increases the EAF and EAI and the effect is much greater in the EAF with 35% variation in the NF ground motions.

Referring to Tables (7) and (8), it is evident that the modeling uncertainty has no effect on the EAF of archetypes but increases other performance measures. Figure (5) shows percentage change of performance parameters in I-IMF-Heat archetypes because of modeling uncertainty. It can be seen and the effect of modeling uncertainty increases for the NF ground motions comparing with FF ground motions for normalized EAL, but the variation in other parameters are nearly equal. Maximum percentage change in EAL considering modeling uncertainty is for I-IMF-Heat in the NF ground motions with 20.8% variation; therefore, modeling uncertainty has a great effect on performance parameters.

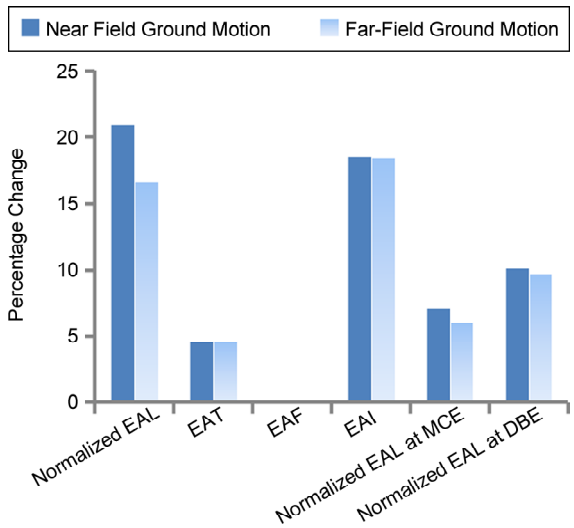

Figure 5. Percentage change of performance parameters in I-IMF-Heat archetypes because of modeling uncertainty.

4. Conclusion

This study utilizes performance-based seismic design and loss assessment methodology based on FEMA P-58 [1] to investigate seismic performance of inelastic isolated structures considering heating in lead core subject to set of far and near-field ground motion records in terms of collapse risk and human and financial losses. PBSD provides a useful framework for developing an understanding of the relationships among the characteristics of the ground motion, superstructure and isolation system, and to evaluate the ability of various design approaches and isolator system properties to reliably achieve targeted performance goals.

Finding of collapse assessments show that the effect of heating in lead core on collapse fragility under far-field ground motions in low spectral accelerations is negligible, but in high spectral accelerations this effect is remarkable. In addition, the effect of heating in lead core in collapse fragility under near-field ground motions for all range of spectral acceleration is considerable but in high spectral acceleration this effect is reduced. Furthermore, heating in lead core leads to increase of annual frequency of collapse by 30% under far-field ground motions and 40% under near-field ground motions, also collapse margin ratio reduces by 10.8% under far-field ground motions and 15.2% under near-field ground motions. Therefore, the effect of heating in lead core on collapse parameters under near-field is greater than far-field earthquakes.

Loss estimation outcomes demonstrate that heating in lead core of isolated archetypes increases expected annual loss because of increasing demand parameters like drifts. This effect increases under near-field ground motions as the percentage change in expected annual loss considering the heating effect are 10.5% and 38.5% under far-field and near-field earthquakes, respectively. Besides, heating in lead core of isolation system increases expected annual fatalities and expected annual injuries and the effect is much greater in expected annual fatalities with 35% variation in near-field ground motions. Sensitivity analysis to consider the effect of modeling uncertainty on the loss estimation process show that the effect of modeling uncertainty on expected annual loss increases for near-field ground motions comparing with far-field ground motions.

It should be noted that differences in the employed population models, hazard analysis results and collapse performance of the studied buildings lead to different performance parameters. Therefore, in order to reach to a more comprehensive conclusion, sets of archetypes designed with different heights, various structural systems, different population models and zones with different levels of seismic hazard have to be evaluated.

The benefit of loss estimation approach is an improved method to assess the effect of heating in lead core on isolation system performance in terms of human and financial losses and can provide stakeholders and insurance companies with measures to assess the seismic risk.

References

1. FEMA P-58 (2012) *Seismic Performance Assessment of Buildings*. Federal Emergency Management Agency (FEMA), Washington, DC.

2. Moehle, J. and Deierlein, G.G. (2004) A framework methodology for performance-based earthquake engineering. *13th World Conference on Earthquake Engineering*, Vancouver, Canada, Paper No: 679.

3. Alhamaydeh, M.H., Barakat, S.A., and Abed, F.H. (2013) Multiple regression modeling of natural rubber seismic-isolation systems with supplemental viscous damping for near-field ground motion. *Journal of Civil Engineering and Management*, **19**(5), 665-682.

4. Villaverde, R. (2011) Recent advances in base isolation technology. *Journal of Seismology and Earthquake Engineering*, **13**(3-4), 209-218.

5. Naeim, F. and Kelly, J.M. (1999) *Design of Seismic Isolated Structures: from Theory to Practice*. John Wiley, California.

6. Goda, K., Lee, C.S., and Hong, H.P. (2010) Lifecycle cost-benefit analysis of isolated buildings. *Structural Safety*, **32**(1), 52-63.

7. Fathi, M., Makhdoumi, A., and Parvizi, M. (2015) Effect of supplemental damping on seismic response of base isolated frames under near and far field accelerations. *KSCE Journal of Civil*

Engineering, **19**(5), 1359-1365.

8. Kalpakidis, I.V., Constantinou, M.C., and Whittaker, A.S. (2010) Modeling strength degradation in lead-rubber bearings under earthquake shaking. *Earthquake Engineering and Structural Dynamics*, **39**(13), 1533-1549.

9. Morgan, T.A. and Mahin, S.A. (2011) *The Use of Base Isolation Systems to Achieve Complex Seismic Performance Objectives*. Report Pacific Earthquake Engineering Research Center, College of Engineering, University of California, Berkeley.

10. Krawinkler, H., Zareian, F., Medina, R.A., and Ibarra, L.F. (2006) Decision support for conceptual performance-based design. *Earthquake Engineering and Structural Dynamics*, **35**(1), 115-133.

11. Williams, R.J., Gardoni, P., and Bracci, J.M. (2009) Decision analysis for seismic retrofit of structures. *Structural Safety*, **31**(2), 188-196.

12. ASCE/SEI 7-10 (2010) *Minimum Design Loads for Buildings and other Structures*. American Society of Civil Engineers (ASCE), Reston, Virginia.

13. ANSI/AISC 360-10 (2010) *Specification for Structural Steel Buildings*. American Institute of Steel Construction (AISC), Chicago, IL.

14. ANSI/AISC 341-10 (2010) *Seismic Provisions for Structural Steel Buildings*. American Institute of Steel Construction (AISC), Chicago, IL.

15. Erduran, E., Dao, N.D., and Ryan, K.L. (2011) Comparative response assessment of minimally compliant low-rise conventional and base-isolated steel frames. *Earthquake Engineering and Structural Dynamics*, **40**(10), 1123-1141.

16. Sayani, P.J., Erduran, E., and Ryan, K.L. (2010) Comparative response assessment of minimally compliant low-rise base-isolated and conventional steel moment-resisting frame buildings. *Journal of Structural Engineering*, **137**(10), 1118-1131.

17. Kazantzi, A.K., Vamvatsikos, D., and Lignos, D.G. (2014) Seismic performance of a steel moment-resisting frame subject to strength and ductility uncertainty. *Engineering Structures*, **78**, 69-77.

18. Ibarra, L.F., Medina, R.A., and Krawinkler, H. (2005) Hysteretic models that incorporate strength and stiffness deterioration. *Earthquake Engineering and Structural Dynamics*, **34**(12), 1489-1512.

19. Lignos, D.G. and Krawinkler, H. (2010) Deterioration modeling of steel components in support of collapse prediction of steel moment frames under earthquake loading. *Journal of Structural Engineering*, **137**(11), 1291-1302.

20. Vamvatsikos, D. and Cornell, C.A. (2002) Incremental dynamic analysis. *Earthquake Engineering and Structural Dynamics*, **31**(3), 491-514.

21. FEMA P695 (2009) *Quantification of Building Seismic Performance Factors*. Federal Emergency Management Agency (FEMA), Washington, DC.

22. Kumar, M., Whittaker, A.S., and Constantinou, M.C. (2014) An advanced numerical model of elastomeric seismic isolation bearings. *Earthquake Engineering and Structural Dynamics*, **43**(13), 1955-1974.

23. Liel, A.B. (2008) *Assessing the Collapse Risk of California's Existing Reinforced Concrete Frame Structures: Metrics for Seismic Safety Decisions*. Ph.D. Thesis, Department of Civil and Environmental Engineering, Stanford University, California, United States.

24. hokrabadi, M., Banazadeh, M., Shokrabadi, M., and Mellati, A. (2015) Assessment of seismic risks in code conforming reinforced concrete frames. *Engineering Structures*, **98**, 14-28.

25. Erberik, M.A. and Elnashai, A.S. (2006) Loss estimation analysis of flat-slab structures. *Natural Hazards Review*, **7**(1), 26-37.

26. Parvini Sani, H. and Banazadeh, M. (2012) Decision analysis for seismic retrofit based on loss estimation. *15th World Conference on Earthquake Engineering*, Lisbon, Portugal.

27. Banazadeh, M., Gholhaki, M., and Parvini Sani,

H. (2016) Cost-benefit analysis of seismic-isolated structures with viscous damper based on loss estimation. *Structure and Infrastructure Engineering*, Published Online 26 Sep 2016.

28. Bozorgnia, Y. and Bertero, V.V. (2004) *Earthquake Engineering: from Engineering Seismology to Performance-Based Engineering*. CRC Press, Boca Raton, F.L.

29. Charette, R.P. and Marshall, H.E. (1999) *UNIFORMAT II Elemental Classification for Building Specifications, Cost Estimating, and Cost Analysis*. National Institute of Standards and Technology, United States.

30. Dyanati, M., Huang, Q., and Roke, D. (2015) Life cycle cost-benefit evaluation of self-centering and conventional concentrically braced frames. *12th International Conference on Applications of Statistics and Probability in Civil Engineering, Vancouver*, Canada, Paper No: 424.